Experiments in Fluids (2006) 40: 753–763
DOI 10.1007/s00348-006-0112-2

RESEARCH ARTICLE

H. Hu · M. Koochesfahani · C. Lum

Molecular tagging thermometry with adjustable temperature sensitivity

Received: 19 April 2005 / Revised: 4 January 2006 / Accepted: 5 January 2006 / Published online: 7 February 2006

Abstract We report an extension to the technique of molecular tagging thermometry which allows for adjustable temperature sensitivity. The temperature dependence of laser-induced phosphorescence of the water-soluble phosphorescent triplex (1-BrNp•Mβ-CD•ROH) is used to conduct temperature measurements in aqueous flows. It is shown that the temperature sensitivity of phosphorescence intensity can be adjusted by changing the time delay between the laser excitation pulse and the start of the phosphorescence emission acquisition. For example, for a phosphorescence integration period of 1 ms, the temperature sensitivity of the measured phosphorescence intensity varies in the range 8.15–18.2% per °C at 25°C as the time delay changes from 1 to7 ms. This temperature sensitivity is much higher than that of most fluorescent dyes used for temperature measurements (e.g. less than about 2% per °C for Rhodamine B). The implementation and application of this new approach are demonstrated by conducting temperature measurements in the wake of a heated cylinder.

1 Introduction

Fluorescence and phosphorescence are molecular photoluminescence phenomena that are often used for imaging in science and engineering. The general properties of these processes can be found in texts on photochemistry (e.g. Turro 1978; Ferraudi 1988). Fluorescence refers to the radiative process when a molecule transitions from a singlet excited state to its singlet ground state. Since singlet–singlet transitions are quantum mechanically allowed, they occur with a high probability, making fluorescence short-lived with short emission lifetimes of the order of nanoseconds. Phosphorescence, on the other hand, is a radiative process when a molecule transitions from a triplet excited state to its singlet ground state. Because such transitions are quantum mechanically forbidden, phosphorescence is long-lived with emission lifetimes that may approach milliseconds to minutes.

For dilute solutions and unsaturated laser excitation energies, the total photoluminescence (either fluorescence or phosphorescence) emission intensity I at a given point is given by

$$I = AI_{\mathrm{i}}C\varepsilon\Phi, \tag{1}$$

where A is a parameter representing the detection collection efficiency, I_{i} the local incident laser intensity, C the concentration of the dye, ε the absorption coefficient, and Φ the photoluminescence quantum efficiency. For some molecules, the absorption coefficient ε and/or the quantum efficiency Φ are temperature dependent, allowing the measurement of the emission intensity of tracer molecules to be used to quantify the temperature field in a fluid flow. The temperature sensitivity of the measurement can be defined as the rate of change of emission intensity with temperature, i.e. $\partial I/\partial T$.

Laser induced fluorescence (LIF) techniques have been widely used for fluid flow temperature measurements in recent years. The temperature sensitive fluorescent dye, Rhodamine B, has been one of the most common tracers used in various applications (Sakakibara et al. 1993; Sato et al. 1997; Coppeta and Rogers 1998; Sakakibara and Adrian 1999; Kim and Khim 2001; Lavieille et al. 2001). Coppeta and Rogers (1998) and Saeki and Hart (2001) conducted comparative studies of commonly used fluorescent dyes in liquids, and found that Rhodamine B is the one with the highest

H. Hu (✉)
Department of Aerospace Engineering, Iowa State University, Ames, IA 50011, USA
E-mail: huhui@iastate.edu

M. Koochesfahani · C. Lum
Department of Mechanical Engineering, Michigan State University, East Lansing, MI 48824, USA
E-mail: koochesf@egr.msu.edu

temperature sensitivity among the fluorescent dyes compared. According to data summarized in Table 1, the temperature sensitivity of Rhodamine B fluorescence emission excited at various wavelengths is at best about −2% per °C , i.e., the fluorescence intensity decreases about 2% for every 1°C increase in temperature. This relatively low temperature sensitivity makes accurate temperature measurements rather challenging in engineering applications where the temperature differences in a fluid flow are quite small (e.g. only a few degrees). In these situations, one would have to resort to very low-noise, high dynamic range detectors (e.g. 16 bits), or use other thermometry methods such as the particle-encapsulated liquid crystal approach (Dabiri and Gharib 1991). It would be desirable to develop a molecular-based thermometry technique that can provide a much higher temperature sensitivity compared to that currently offered by fluorescent dyes. In this paper, we present one such method which relies on using a phosphorescent tracer.

Since the fluorescence emission has a very short lifetime of the order of nanoseconds, LIF methods typically rely on the information obtained from the ''intensity axis'' of the emission process. The fluorescence emission is usually acquired while the laser excitation is still illuminating the flow, leading to potential contamination of the LIF signal by the reflection and/or scattering of the incident laser light. The use of optical filters to mitigate this problem results in a reduction of the LIF signal because the Stokes shift (i.e. shift in wavelength towards red) between the absorption and fluorescence emission spectra is usually small. Depending on the extent of the Stokes shift, it is sometimes very difficult to eliminate these contaminations completely. Use of phosphorescent tracers, as reported in this paper, can offer certain advantages for imaging in fluid flows. The Stokes shift in phosphorescence is typically much larger than that in fluorescence and it is easy to filter out the artifacts caused by the excitation source. In addition, the relatively long lifetime of phosphorescence allows one to take advantage of the ''time axis'' in the emission process. For example, when excited by a pulsed laser, recording the phosphorescence emission with a slight time delay after the laser pulse, can be used to effectively eliminate the artifacts (i.e. scattering, reflection) caused by the intense excitation source. As will be shown in this paper, by adjusting this time delay we can also increase the sensitivity of temperature measurements based on phosphorescence emission.

A difficulty in using phosphorescent tracers is that long-lived excited states suffer from O_2 quenching, and as a result suitable molecular complexes have not been available for aqueous flows until recently. It has been shown that water-soluble supramolecular complexes may be designed to exhibit long-lived phosphorescence, which is not quenched, upon mixing a lumophore, an appropriate alcohol, and cyclodextrin (Ponce et al. 1993; Mortellaro and Nocera 1996; Hartman et al. 1996). A successful design, which has found extensive use as a tracer for Molecular Tagging Velocimetry (Koochesfahani et al. 1996; Gendrich et al. 1997), is 1-BrNp•Gβ-CD•ROH, a triplex formed by mixing the lumophore (1-BrNp), certain alcohols (indicated collectively by ROH), and an aqueous solution of glucosyl-β-cyclodextrin, Gβ-CD. The resulting long-lived green phosphorescence has a typical lifetime of up to several milliseconds. The use of this phosphorescent triplex for thermometry was first reported by Thomson and Maynes (2001) who coined the term molecular tagging thermometry (MTT). In that work, the variation of phosphorescence intensity with temperature was used as the basis for thermometry. By taking advantage of the temperature dependence of the phosphorescence lifetime, Hu and Koochesfahani (2003) developed a lifetime-based thermometry technique, a *ratiometric* approach to eliminate the effects of the variations in the incident laser intensity and the non-uniformity of the dye concentration.

In this paper, an extension to MTT is presented which allows for an adjustable sensitivity in temperature measurement. The temperature sensitivity is adjusted by simply changing the time delay between phosphorescence emission acquisition and the excitation laser pulse. This approach is shown to provide about ten times higher sensitivity compared with most fluorescent dyes used for LIF temperature measurements (e.g. about 2.0% per °C for Rhodamine B). Because of the time delay, the method also effectively eliminates the potential artifacts caused by the reflection and scattering of the intense incident laser light. In the sections that

Table 1 The temperature sensitivity of the fluorescence emission of Rhodamine B excited at different wavelengths

	$\lambda_{excitation}$ = 308 nm (excimer laser)	$\lambda_{excitation}$ = 488 nm (argon ion laser)	$\lambda_{excitation}$ = 514 nm (argon ion laser)	$\lambda_{excitation}$ = 532 nm (Nd:Yag laser)
Coppeta and Rogers (1998)	–	–	−1.54% per °C (20°C–60°C)	–
Sakakibara and Adrian (1999)	–	−1.95% per °C (15°C ~ 40°C)	–	–
Saeki and Hart (2001)	–	–	–	−1.34% per °C (25°C–85°C)
Kim and Khim (2001)	–	−1.35 % per °C (16°C ~ 40°C)	–	–
Present study (Fig. 5)	−1.55% per °C (6°C–66°C)	-	–	–

follow, the technical basis and implementation of the new technique are described, along with a demonstration experiment involving temperature measurements in the wake of a heated cylinder.

2 Description of the experimental technique

The work described here is based on the laser induced phosphorescence of the triplex 1-BrNp•Mβ-CD•ROH, even though the underlying basis of the approach is general and applicable to other phosphorescent compounds. In this triplex, the original glucose sugar subunits that are hanging off the rim of the cyclodextrin for increased solubility (i.e. glucosyl-β-cyclodextrin, Gβ-CD) have been replaced by maltose (i.e. maltosyl-β-cyclodextrin, Mβ-CD). The measured properties of both glucose- and maltose-based triplexes were found to be quite similar and the two can be used interchangeably. The alcohol used here was cyclohexanol. The molar concentrations of the three constituents of the triplex were according to those recommended by Gendrich et al. (1997), i.e. 2×10^{-4} M for Mβ-CD, approximately 1×10^{-5} M for 1-BrNp (a saturated solution), and 0.06 M for the alcohol. Figure 1a shows the normalized absorption and emission spectra of the phosphorescent triplex 1-BrNp•Mβ-CD•ROH. The fluorescence and phosphorescence spectra are both shown and, as described before, the phosphorescence emission is significantly red-shifted relative to fluorescence. Also note that because of this large red shift in this figure, there is no overlap between the phosphorescence emission and absorption spectra and the phosphorescence does not get re-absorbed. Figure 1b shows the emission spectra of the 1-BrNp•Mβ-CD•ROH solution at different temperatures. It is seen in this figure that the phosphorescence emission of this triplex is very temperature sensitive, whereas its fluorescence is not. The fluorescence lifetime of the triplex is within 20 ns, while its phosphorescence lifetime is about 5.0 ms at 20°C and decreases with increasing temperature (Hu and Koochesfahani 2003).

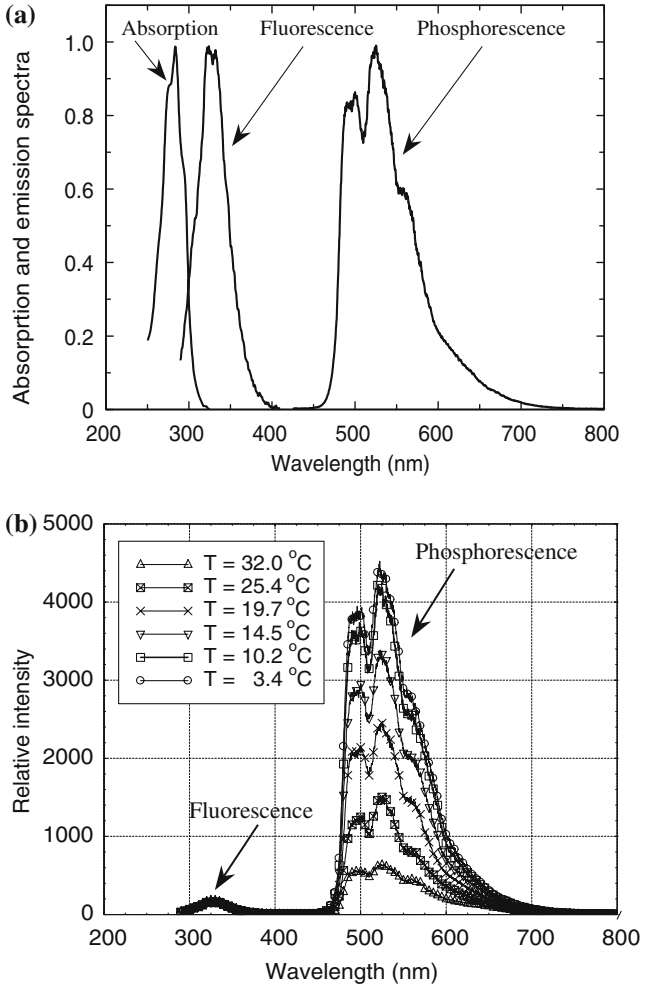

Fig. 1 Absorption and emission spectra of the 1-BrNp•Mβ-CD•ROH complex. **a** Normalized absorption and emission spectra at room temperature. **b** Emission spectra at different temperatures (280 nm excitation of spectrophotometer)

According to Quantum theory (Pringsheim 1949), the intensity of the photoluminescence process (either flourescence or phosphorescence) decays exponentially. For the sake of simplicity, only a single-exponential process is considered here. However, the methodology described in this study is also applicable to multiple-exponential processes. The emission intensity decay can be expressed in the form

$$I_{\mathrm{em}} = I_{\mathrm{o}}\, \mathrm{e}^{-t/\tau}, \tag{2}$$

where the lifetime τ refers to the time when the intensity drops to 37% (i.e. $1/e$) of the initial intensity I_{o}. The total phosphorescence intensity given in Eq. 1 can also be separately determined from the integration of Eq. 2 over all time, resulting in

$$I_{\mathrm{p}} = \tau\, I_o, \tag{3}$$

where subscript $()_{\mathrm{p}}$ is used to denote phosphorescence. Comparing Eq. 1 and 3 leads to

$$I_{\mathrm{o}} = A\, I_{\mathrm{i}}\, \varepsilon\, \Phi_{\mathrm{p}}\, C/\tau. \tag{4}$$

Now consider capturing the phosphorescence emission by a gated intensified CCD detector, where the integration starts at a delay time t_{o} after the laser excitation pulse with an integration (or gate) period of Δt (see Fig. 2). The phosphorescence signal S_{p} collected by the detector is then given by

$$S_{\mathrm{p}} = \int_{t_{\mathrm{o}}}^{t_{\mathrm{o}}+\Delta t} I_{\mathrm{o}} \mathrm{e}^{-t/\tau} \mathrm{d}t \;=\; I_{\mathrm{o}}\, \tau \left(1 - \mathrm{e}^{-\Delta t/\tau}\right) \mathrm{e}^{-t_{\mathrm{o}}/\tau}. \tag{5}$$

Using the equations given above, it can be shown that

$$S_{\mathrm{p}} = A\, I_{\mathrm{i}}\, C\, \varepsilon\, \Phi_{\mathrm{p}} \left(1 - \mathrm{e}^{-\Delta t/\tau}\right) \mathrm{e}^{-t_{\mathrm{o}}/\tau}. \tag{6}$$

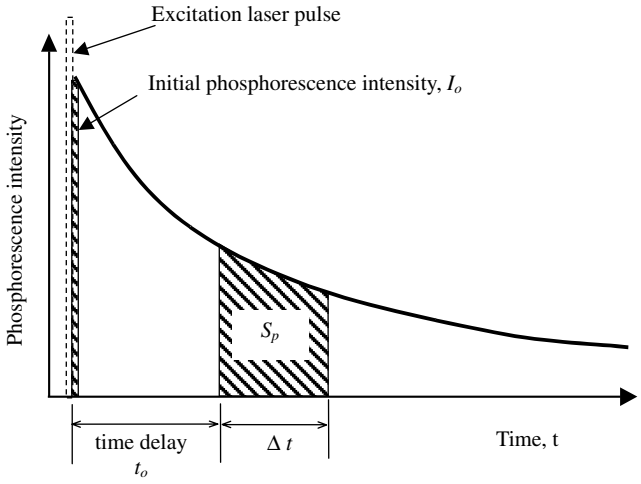

Fig. 2 Timing chart for phosphorescence image acquisition. The phosphorescence signal S_p is acquired at a delay time t_o after the laser excitation pulse with an integration period of Δt

The absorption coefficient ε, phosphorescence quantum yield Φ_p, and the phosphorescence lifetime τ are in general temperature-dependent, resulting in a temperature-dependent phosphorescence signal S_p, according to Eq. 6. Thus, the phosphorescence signal may, in principle, be used to measure the temperature if the incident laser intensity and the concentration of the phosphorescent dye remain constant (or are known) in the measurement region. This is the approach taken in the original work of Thomson and Maynes (2001), where they quantified the temperature using the phosphorescence intensity of 1-BrNp•Gβ-CD•ROH acquired with a short fixed time delay (8 μs) after the laser pulse. To circumvent the challenges faced by such an intensity-based method, e.g. the variation of the incident laser intensity would have to be corrected separately for quantitative measurements, Hu and Koochesfahani (2003) developed a lifetime-based thermometry technique which takes advantage of the temperature dependence of the phosphorescence lifetime. This approach is *ratiometric* and can eliminate the effects of the variations of the incident laser intensity and the nonuniformity of the phosphorescent dye concentration in the measurement region. The calibration profiles given by Thomson and Maynes (2001) indicate a temperature sensitivity of about 3.0% per °C , whereas the temperature sensitivity of the lifetime-based thermometry technique of Hu and Koochesfahani (2003) is about 5.0% per °C.

The method we describe here, relies on adjusting the time delay between the acquisition of phosphorescence emission and the excitation laser pulse in order to accomplish higher and adjustable temperature sensitivity. Considering the formulation in Eq. 5, we note that the phosphorescence initial intensity I_o and lifetime τ are both dependent on temperature. Using a reference temperature T_{ref} , and its corresponding phosphorescence signal $(S_p)_{ref}$, the relative phosphorescence signal R can be defined as the ratio of the signal at temperature T to that at T_{ref}, given below

$$R = \frac{S_p}{(S_p)_{ref}} = \frac{I_o(T)\,\tau(T)\left(1-e^{-\Delta t/\tau(T)}\right)}{I_o(T_{ref})\,\tau(T_{ref})\left(1-e^{-\Delta t/\tau(T_{ref})}\right)}\, e^{-(t_o/\tau(T)-t_o/\tau(T_{ref}))} \propto R(T,\Delta t, t_o). \quad (7)$$

From Eq. 7 we observe that the relative phosphorescence signal R is a function of the variable we wish to measure, i.e. temperature T, and two experimentally controllable parameters, the gate/exposure period Δt, and the time delay t_o between signal acquisition and the excitation laser pulse. For a fixed set of (Δt, t_o) values, Eq. 7 defines a unique relation between R and T which can be used for thermometry. More importantly, however, is the fact that R is also a function of two controllable parameters and the sensitivity of temperature measurement, $\partial R/\partial T$, can be adjusted by the choice of those parameters. The next section will give the details of the calibration procedure for R and the range of sensitivities that can be achieved with the phosphorescent triplex 1-BrNp•Mβ-CD•ROH.

To summarize, the thermometry approach presented would involve an experimental procedure where the excitation laser pulse fires first, followed by capturing the phosphorescence image at a time delay t_o after the laser pulse. The phosphorescence image is then normalized by a previously-acquired reference image in order to determine the relative phosphorescence response, resulting in the estimate of the temperature using the calibration curve for the temperature dependence of R in Eq. 7. In using this procedure, it is important to recognize that the relative phosphorescence response R , described by Eq. 7, takes into account only the temperature response of the phosphorescence signal. Other influences that affect the initial intensity I_o, such as temporal or spatial variations of the incident laser intensity, or possible changes in the dye concentration (e.g. due to bleaching during the experiment), need to be separately accounted for. In the demonstration experiment described in Sect. 4, the spatial nonuniformity of the incident laser sheet illumination is corrected for and dye bleaching is rendered negligible by the combination of a relatively large volume of the flow system and a short exposure to laser light. The temporal variation of the laser intensity, i.e. the pulsed laser shot-to-shot energy variation, is not accounted for, however, and its effect is included in the accuracy measures that will be presented. Therefore, the demonstration experiment that will be presented still uses an intensity-based approach. In the discussion in Sect. 4, two possibilities will be presented for extending the present measurement method into a ratiometric approach that will automatically account for incident intensity variations and possible bleaching effects.

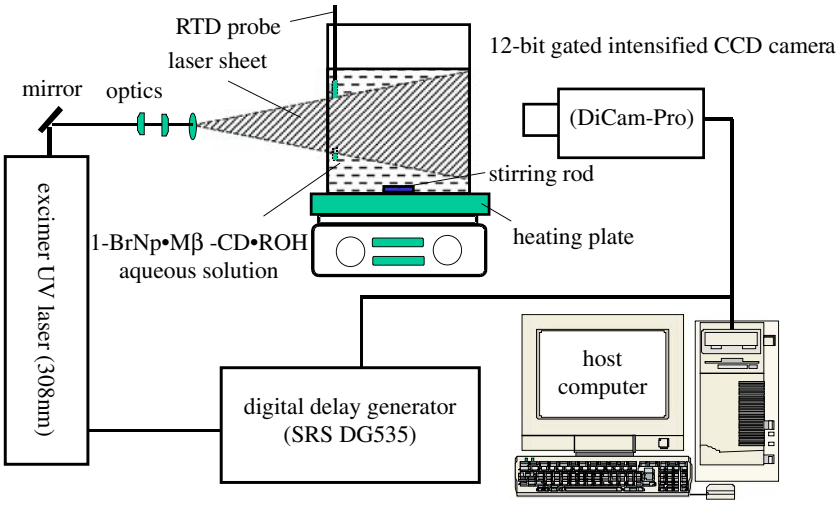

Fig. 3 The schematic setup for the calibration procedure

3 Calibration procedure

Figure 3 shows the schematic setup of the calibration procedure employed to quantify the relative phosphorescence signal R, defined in Eq. 7, for 1-BrNp•Mβ-CD•ROH. A Lambda Physik XeCl excimer laser (wavelength $\lambda = 308$ nm, energy 100 mJ/pulse, pulse width 20 ns) with appropriate optics was used to generate a laser sheet (thickness about 1 mm) to illuminate a cube-shaped test cell (about 2 l in volume) containing an aqueous solution of 1-BrNp•Mβ-CD•ROH complex. The apparatus was placed on a heating plate and a stirring rod was used to achieve thermal equilibrium in the test cell. An RTD probe (Hart Scientific Model 1502A, temperature accuracy ± 0.01°C) was placed in one corner of the apparatus to measure the actual temperature in the test cell. During the experiment, the temperature uniformity inside the test cell was checked and was found to be within 0.1°C.

A 12-bit, 1,280 × 1,024 pixels, gated intensified CCD camera (PCO DiCam-Pro) with a fast decay phosphor (P46) was used to capture the phosphorescence emission. The laser and the camera were synchronized using a digital delay generator (SRS DG535), which controlled the delay time t_o between the laser pulse and the start of image capture, and the integration period Δt. The phosphorescence images were subsequently transferred to a host computer for analysis. In the present study, the exposure time was set to a fixed value of $\Delta t = 1$ ms.

To acquire the calibration data, the aqueous solution of 1-BrNp•Mβ-CD•ROH was first heated to a predetermined temperature level. After thermal equilibrium was established, the phosphorescence images were acquired as a function of time delay t_o. The process was repeated for different solution temperatures. Figure 4 depicts the measured phosphorescence intensity decay curves at several temperature levels. It can be seen that these phosphorescence decay curves are very well approximated by single-exponential curves, as expected theoretically. Using the data in Fig. 4 and normalizing them with the data at a reference temperature T_{ref} yields the relative phosphorescence signal $R(T, \Delta t, t_o)$. The results shown in Fig. 5 are based on an arbitrarily selected reference temperature $T_{ref} = 25.0$°C and illustrate the variation of R with temperature T for different time delays t_o. As indicated previously, the exposure time was maintained at a fixed value of $\Delta t = 1$ ms throughout this study. For comparison, Fig. 5 also includes the variation of Rhodamine B fluorescence emission with temperature measured in the same calibration setup and using excimer laser excitation at 308 nm wavelength.

Recognizing that the decay slope $\partial R/\partial T$ of the calibration profiles in Fig. 5 represents the temperature measurement sensitivity, several aspects of the data in this figure are noteworthy. It can be seen that thermometry based on phosphorescence of 1-BrNp•Mβ-CD•ROH is generally much more sensitive than fluorescence of Rhodamine B, with the differences becoming more significant at higher temperatures. It is also found that the temperature measurement sensitivity can be changed by adjusting the time delay t_o between the laser

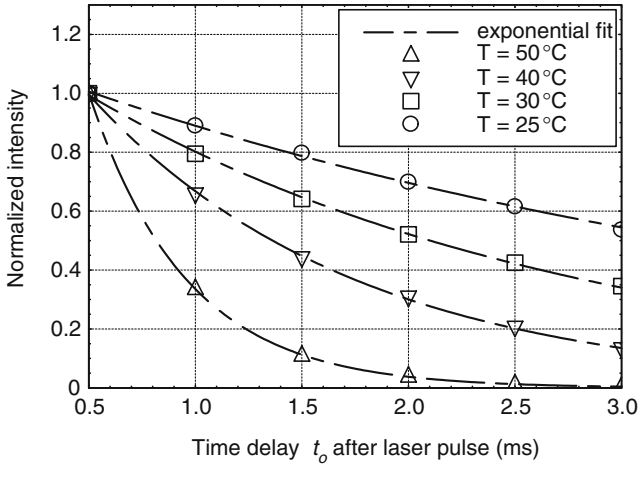

Fig. 4 Phosphorescence intensity decay curves at several temperature levels

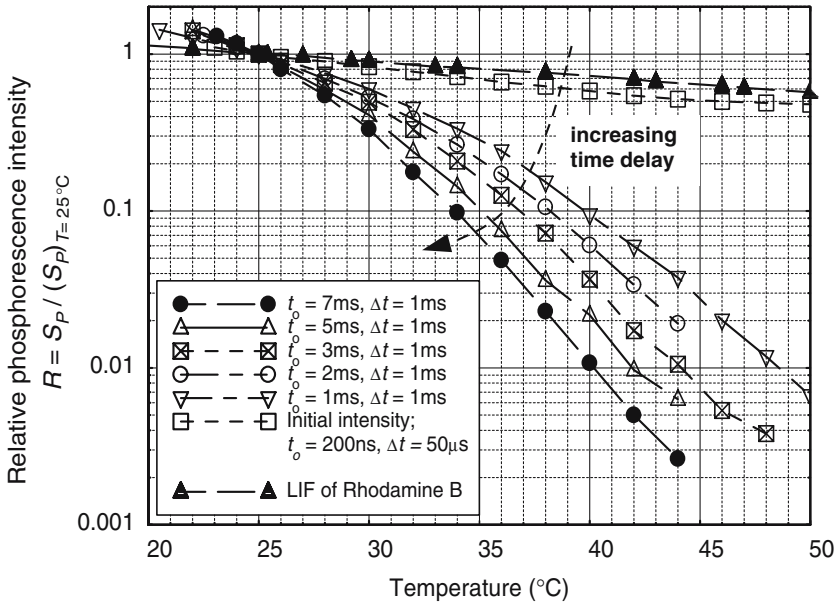

Fig. 5 The calibration profiles in terms of the measured relative phosphorescence signal R versus time delay t_o

pulse and the start of phosphorescence acquisition. As the time delay becomes longer, the sensitivity becomes higher. Based on the calibration profiles in Fig. 5, the temperature sensitivity $\partial R/\partial T$ can be calculated. Results are tabulated in Table 2 in terms of percent sensitivity at $T = 25°C$, i.e. percent change in signal for 1°C change in temperature calculated according to $[(1/R)(\partial R/\partial T)]$. These results show that the measurement sensitivity is 8.15% per °C with a 1 ms time delay and increases to 18.2% per °C as the delay time is lengthened to 7 ms. These sensitivity values are significantly higher than the temperature sensitivity of Rhodamine B fluorescence (1.55% per °C at $T = 25°C$, 308 nm excitation).

Figure 5 indicates that the sensitivity of temperature measurement continuously increases as the delay time t_o between the laser pulse and the start of phosphorescence image capture gets longer. In principle, it should be possible to reach any desired temperature sensitivity if the delay time is set to be long enough. However, as delay times get longer, the exponentially decaying phosphorescence emission (see Fig. 4) would necessitate the use of high-gain detectors (e.g. intensified cameras) to capture the resulting weak phosphorescence signal. The signal-to-noise ratio of detection would determine the longest practical delay time that can be used, and the corresponding temperature range that can be achieved. In other words, there is a trade-off between sensitivity and temperature range for a given detector.

Signal to noise characteristics of detection are, of course, specific to each particular detector. For the intensified camera used here, Table 3 provides a summary of the measured temperature uncertainty for different delay times. Using 300 realizations of the measured temperature field in the wake of a heated cylinder (see description of the demonstration experiment in Sect. 4), the temperature uncertainty values (in °C rms) were obtained based on the portion of the data in the freestream region of the wake and comparing them with the known freestream temperature measured independently with a thermocouple probe. Temperature uncertainty results are given both for a single pixel and a 5 × 5 pixels averaging region which is used here to reduce the measurement uncertainty. An important result from Table 3 is that the measurement uncertainty does

Table 2 The temperature sensitivities of the phosphorescence emission of the 1-BrNp•Mβ-CD•ROH complex at 25°C

Time delay t_o after laser pulse	t_o = 1.0 ms	t_o = 2.0 ms	t_o = 3.0 ms	t_o = 5.0 ms	t_o = 7.0 ms
Temperature sensitivity	8.15% per °C	10.0 % per °C	13.0% per °C	16.2% per °C	18.2% per °C

The exposure time for the phosphorescence acquisition was 1 ms

Table 3 The temperature measurement uncertainty (°C rms) in the freestream region of the cylinder wake in the demonstration experiment (sample size = 300)

Time delay t_o after laser pulse	t_o = 1.0 ms	t_o = 3.0 ms	t_o = 5.0 ms	t_o = 7.0 ms
Temperature uncertainty for 1×1 pixel region	0.52°C	0.42°C	0.43°C	0.46°C
Temperature uncertainty for 5×5 pixel region	0.44°C	0.29°C	0.28°C	0.29°C
Temperature uncertainty resulting from a 3.3% laser energy fluctuation	0.39°C	0.25°C	0.20°C	0.18°C

The camera intensifier gain was not held fixed as the time delay increased

not increase as the time delay gets longer. Interestingly, any increase in the measurement noise is offset by the increase in temperature sensitivity. The accuracy measures described here also include the temporal variation of the laser intensity, i.e. the pulsed laser shot-to-shot energy variation. The contribution of laser intensity fluctuation (about 3.3% shot-to-shot energy variation) to temperature measurement uncertainty is indicated in Table 3. This part of the overall uncertainty can be removed using a ratiometric approach described in Sect. 4.

4 Demonstration experiment

In order to verify the feasibility and implementation of the MTT technique described above, a demonstration experiment was carried out by conducting temperature measurements in the wake of a heated cylinder.

4.1 Experimental setup and flow conditions

A schematic representation of the experimental setup for the demonstration experiment is shown in Fig. 6. The test cylinder was installed horizontally in a gravity-driven vertical water channel. The dimensions of the test section were 50 mm (width) × 30 mm (height) × 200 mm (length). Two sides of the test section contained quartz windows to allow the transmission of the excimer laser UV light. The 1-BrNp•Mβ-CD•ROH phosphorescent triplex was premixed with water in a reservoir tank. A constant head tank was used to maintain a steady inflow condition during the experiment. The constant head tank was filled from the reservoir tank by using an electric pump. A convergent section with honeycomb and mesh structures was used upstream of the test section to produce a uniform condition for the flow approaching the test cylinder. The velocity of the flow in the water channel was adjustable by operating the valve at the downstream end of the water channel.

A copper tube with an outer diameter of $D = 4.76$ mm and an inner diameter of 4.00 mm was used as the test cylinder. The cylinder was heated using a 3.1 mm diameter rod cartridge heater (Watlow Firerod) that was placed inside the copper tube. High thermal conductivity paste (OMEGATHERM 201) was pressed in to fill the gap between the rod cartridge heater and the inner wall of the copper tube. The rod cartridge heater was powered by a DC power supply (Kepco, BOP-200-2 M). Two J-type thermocouples were embedded in the gap at the mid-span of the cylinder at two angular locations to provide the estimate of the cylinder temperature. The thermocouples were connected to a two-channel thermometer (Omega HH23), which had a resolution of ± 0.1°C.

The 150 mJ/pulse beam from an Excimer UV Laser (308 nm wavelength, 20 ns pulse width) was manipulated by a set of mirrors and cylindrical lenses to generate a laser sheet (thickness about 1 mm) to illuminate

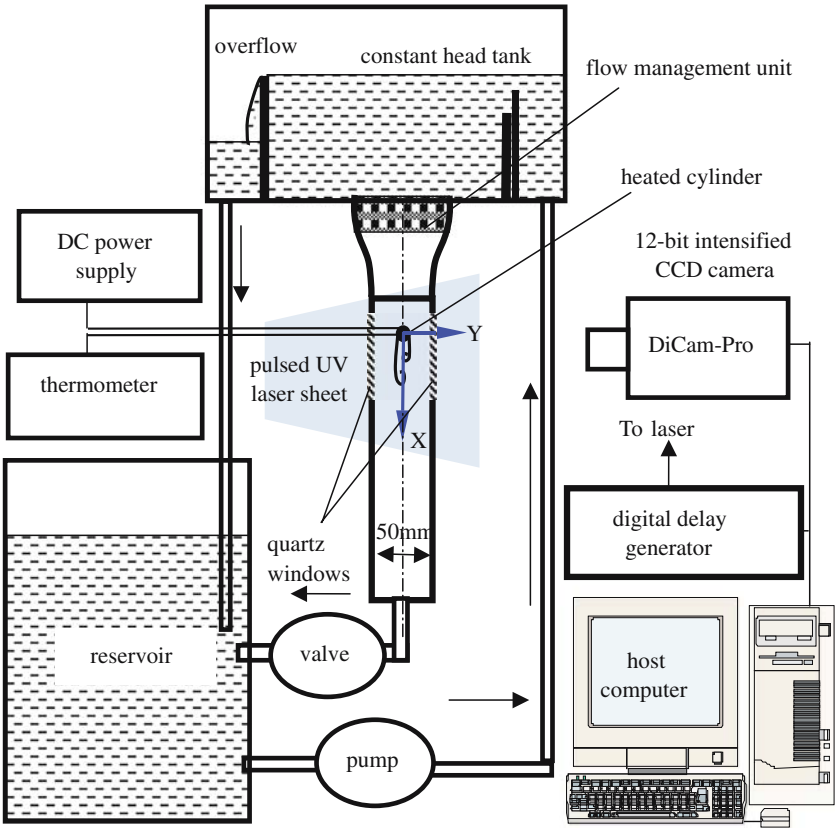

Fig. 6 Experimental setup

the measurement region. The camera and timing electronics arrangement for image acquisition are exactly the same as that previously described for the calibration procedure, with the image acquisition exposure time set at 1 ms. In the present study, the freestream flow velocity measured at about ten diameters upstream of the test cylinder was $U_\infty = 0.034$ m/s and the temperature of the incoming flow was $T_\infty = 23.9°C$. The temperature of the test cylinder was maintained at $T_c = 57.0°C$. Using the properties of water at the temperature of the incoming flow, the flow conditions correspond to a Reynolds number $\mathrm{Re}_D = U_\infty D/\nu = 179$, Grashof number $\mathrm{Gr}_D = g\beta(T_c - T_\infty)D^3/\nu^2 = 10,700$, and Richardson number $\mathrm{Ri}_D = \mathrm{Gr}_D/\mathrm{Re}_D^2 = 0.33$.

4.2 Results and discussion

Figure 7 shows typical phosphorescence images acquired at four different time delays after the excitation laser pulse. The images are different realizations of the flow, but were taken at a similar phase of vortex shedding. The dark bands on the top right of the images are shadows caused by the cylinder blocking the laser sheet. The "dark clusters" in the phosphorescence images downstream of the cylinder correspond to the warm fluid shedding periodically from the hot boundary layer around the heated cylinder. From the comparison of the four images it can be seen that the "dark clusters" become more and more pronounced as the time delay between the laser pulse and phosphorescence acquisition increases. This is due to the fact that increasing the time delay results in higher temperature sensitivity (Fig. 5) and, therefore, a higher intensity contrast between the cold ambient fluid and the warm fluid shed from the cylinder.

The measured calibration profiles shown in Fig. 5 can be used to obtain the quantitative temperature distribution in the wake of the heated cylinder based on phosphorescence images. For this purpose, the phosphorescence image taken at a delay time $t_o = 7$ ms was selected for processing (see Fig. 8a). The procedure described by Eq. 7 in terms of the relative phosphorescence response R takes into account only the temperature response of the phosphorescence signal; it does not account for nonuniformities in the laser sheet illumination. The nonuniformity of the incident laser intensity in the measurement region was calibrated by taking a reference phosphorescence image, shown in Fig. 8b, with an unheated cylinder so that the entire flow was at a uniform ambient temperature of 23.9°C. This reference image was the average of 50 instantaneous realizations acquired at the same time delay as that for the temperature measurements, i.e. 7 ms after the laser pulse. The actual temperature distribution is arrived at by first normalizing the phosphorescence image (Fig. 8a) by the reference image (Fig. 8b) to account for the non-uniformity of the incident laser intensity, and then the corrected image is used to derive the quantitative temperature distribution using the calibration curve given in Fig. 5. The resultant temperature distribution is shown in Fig. 8c.

The temperature map in Fig. 8c shows the overall distribution of the temperature field in the first six diameters behind the heated cylinder. The alternate

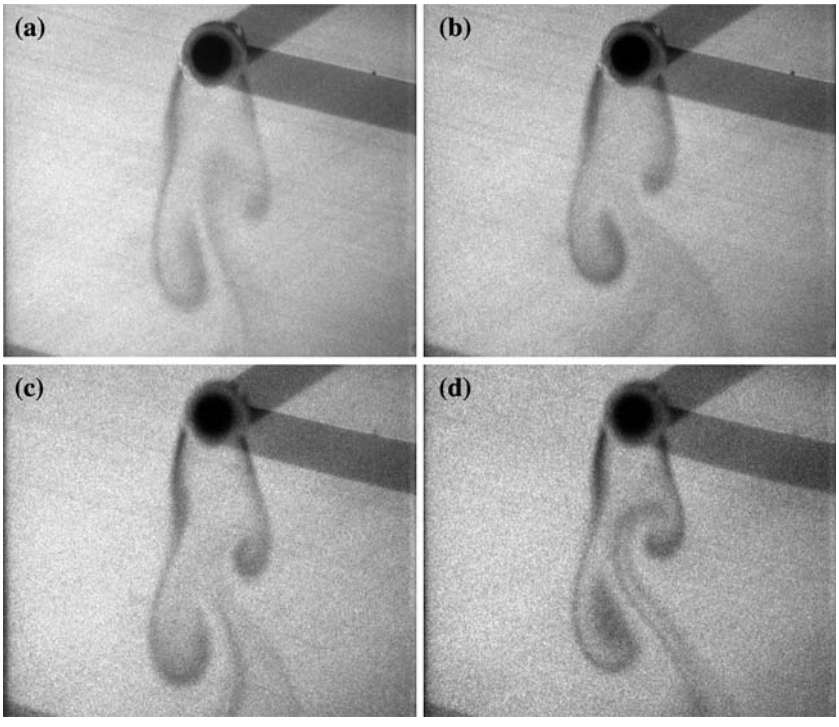

Fig. 7 Comparison of the raw phosphorescence images acquired with different time delay after excitation laser pulse (exposure time $\Delta t = 1$ ms). These images are different realizations at a similar phase of vortex shedding. Flow is *top* to *bottom*. The increase in image graininess with time delay is due to the increased gain of the intensified camera. **a** $t_o = 1$ ms after laser pulse. **b** $t_o = 3$ ms after laser pulse. **c** $t_o = 5$ ms after laser pulse. **d** $t_o = 7$ ms after laser pulse

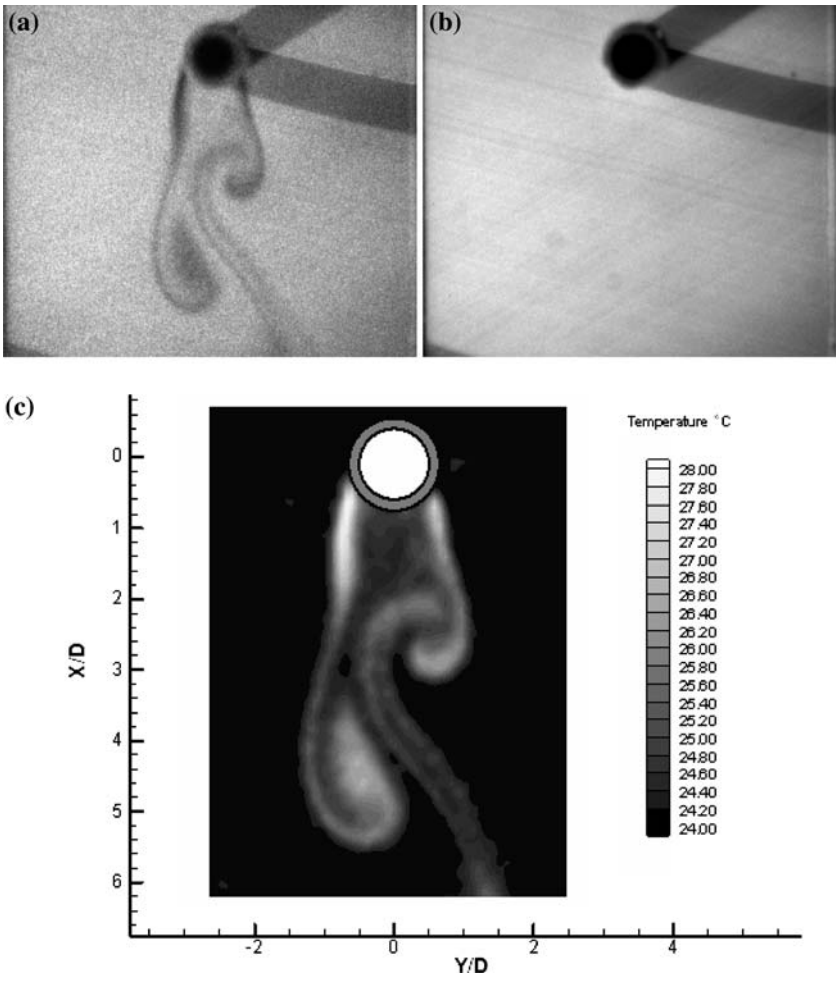

Fig. 8 The raw phosphorescence images and the resultant quantitative instantaneous temperature distribution. **a** Instantaneous phosphorescence image. **b** Excitation laser intensity distribution. **c** The resultant temperature distribution

shedding of warm Karman vortices in the wake is clearly seen, along with the warmer fluid that originates in the hot boundary layer around the heated cylinder. Also seen are the relatively warm braid regions that connect the Karman vortices shedding from the same side of the cylinder. Sample quantitative temperature profiles across the wake at three downtream locations X/D = 1.0, 3.0, 5.0 are extracted from the temperature map of Fig. 8c and the results are shown in Fig. 9. It is observed that the highest temperatures occur in a thin region representing the separating boundary layer near the cylinder. The temperature differences in the wake are quite small for the flow condition studied here, with the maximum reaching only about 4°C above ambient. These small temperature differences are captured here with great detail because of the high temperature sensitivity of the measurement technique. The 4°C temperature difference noted in this flow brings about a 75% intensity variation in the phosphorescence signal. Using 2% per °C as the temperature sensitivity of Rhodamine B fluorescence, the same 4°C temperature difference would have led to only 8% intensity variation in the fluorescence image. The data in Fig. 8c can also be used to estimate the measurement accuracy. Using the portion of the data that fall in the freestream region of the wake (an ensemble of 400 data points) and comparing them with the known ambient temperature of 23.9°C measured independently with a thermocouple probe, it is found that temperature is measured with a 95% confidence limit of ± 0.2°C (or 0.1°C rms). In comparing with the results of Table 3 (second row of data), we note that this accuracy estimate is lower since it is based on spatial data from one realization of the temperature field and does not include the added uncertainty due to the laser intensity fluctuation. For comparison, Sakakibara and Adrian (1999) suggested an accuracy level of about 1.4°C for their work with Rhodamine B fluorescence.

There are several aspects of the measurement technique we have presented that require further clarification and discussion. As presented in its current form, any spatial and temporal variations in the laser sheet illumination field would need to be separately calibrated. The approach adopted here was the same as that commonly used in basic LIF methods; a reference image of the laser illumination field acquired under a uniform temperature condition provided the information to normalize the spatial nonuniformities. This method works well only if the illumination nonuniformities remain spatially and temporally invariant during the experiment, and this requires small variations in the fluid

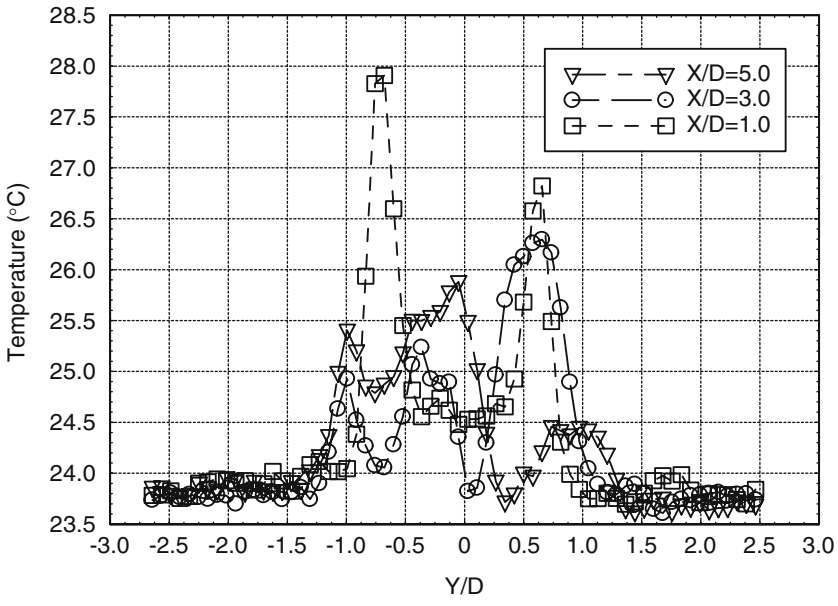

Fig. 9 Quantitative instantaneous transverse profiles of temperature at several downstream locations

index of refraction caused by temperature variations in addition to the spatial and temporal stability of the laser beam intensity distribution. These requirements can be removed if ratiometric methods are used. Ratiometric LIF techniques include the two-color, two-dye approach (e.g. Coppeta and Rogers 1998; Sakakibara and Adrian 1999) and the two-color, one-dye technique (e.g. Lavieille et al. 2001). When using phosphorescence compounds, the ratiometric approach is achieved by direct lifetime-based thermometry (e.g. Hu and Koochesfahani 2003). To extend the measurement method discussed in this paper into a ratiometric approach, two possibilities present themselves. One possibility is to record also the initial phosphorescence signal (see Fig. 5) for each phosphorescence image that is acquired at time delay t_o. This would lead, however, to a slight reduction of the large temperature measurement sensitivities that have been described. An alternate method that should not cause a reduction in sensitivity is to record simultaneously both the fluorescence and the phosphorescence images. According to the emission spectra in Fig. 1, the fluorescence emission of 1-BrNp•Mβ-CD•ROH is almost temperature insensitive and can be used for an in-situ calibration of the laser intensity distribution. A preliminary study has been conducted to verify the feasibility of this idea and further systematic studies are being planned.

The methodology presented here relies on the behavior of the relative phosphorescence signal R (i.e. Fig. 5). The calibration process establishes the relation between R and fluid temperature T based on a constant and uniform temperature environment. Applying these calibration data to thermometry in a real flow environment with nonuniform temperature field should be done with care. Each pixel of the detector integrates the light originating from a finite region in space within which the temperature can be nonuniform, resulting in a nonuniform R within that region. Using the temperature dependence of R in Fig. 5, a procedure can be developed to predict the accuracy of the measured temperature calculated from the calibration curves of Fig. 5 in comparison with the true average temperature within the area imaged onto a pixel. For the measurements presented here, where each pixel mapped into a 50 μm × 50 μm region in the flow, a maximum temperature variation of $\Delta T_{\max} = 1$°C across each pixel (i.e. a spatial temperature gradient of 1°C per 50 μm, or 20°C/mm, in the flow) was estimated to lead to a maximum temperature measurement error of less than 0.04°C. The temperature gradient selected for this estimate is about four times larger than the highest gradient observed in the profiles of Fig. 9. Even though the error is negligibly small for the work described here, one must be aware of it in flows with very large temperature gradients, as the error can be shown to depend quadratically on $\Delta T_{\max}$.

Finally, it should be noted that the molecular tagging thermometry described here is fundamentally different from the LIF thermometry approach in that it is a Lagrangian method. The fluid that is tagged by the excitation laser is interrogated through its phosphorescence at a selected time t_o after the excitation. During this time the fluid convects with the flow which leads to two consequences. The effective spatial resolution of the measurement would have to incorporate, and can become dominated by, the flow displacement. This, of course, makes the effective spatial resolution variable and dependent on the local flow speed. For the measurements presented here, the delay time $t_o = 7$ ms and the freestream flow speed define a spatial resolution of 240 μm. The second consequence is that the fluid "samples" a variable temperature distribution as it convects through a nonuniform temperature field and, similar to the situation described in the previous paragraph, this can lead to potential error between the true

average temperature sampled by the convecting fluid and that estimated using the calibration curves of Fig. 5. These calibration curves and the temperature dependence of phosphorescence lifetime (Hu and Koochesfahani 2003) were used to develop a procedure for estimating the expected error. For the present measurements, the error was calculated to be negligibly small (less than 0.02°C) for a maximum temperature variation of ΔT_{max} = 2°C encountered during flow convection (based on data in Fig. 9). As before, the error can be shown to depend quadratically on ΔT_{max} and one must be aware of it in flows with very large temperature gradients.

5 Conclusions

The development of a methodology was described for MTT with adjustable temperature sensitivity. It was shown that the temperature dependence of laser induced phosphorescence of a water-soluble phosphorescent triplex (1-BrNp•Mβ-CD•ROH) can be used to conduct measurements with a temperature sensitivity as high as 18.2% per °C at 25°C, nearly ten times higher than most fluorescent dyes used for LIF temperature measurements. The implementation and application of this new approach were demonstrated by conducting temperature measurements in the wake of a heated cylinder. Even though the temperature differences in the wake were only about 4°C, the details of the thermal structures shedding periodically from the heated cylinder were clearly revealed. The random error of the temperature measurements in the present study was estimated to be ±0.2°C (95% confidence level). The interplay among the various experimentally-controlled parameters and achievable measurement sensitivities and accuracies were discussed and shown to provide a great deal of flexibility in optimizing the technique for each experiment.

Acknowledgements This work was supported by the CRC Program of the National Science Foundation, Grant Number CHE-0209898, and made use of shared facilities of the MRSEC Program of the National Science Foundation, Award Number DMR-9809688.

References

Coppeta J, Rogers C (1998) Dual emission laser induced fluorescence for direct planar scalar behavior measurements. Exp Fluids 25:1–15

Dabiri D, Gharib M (1991) Digital particle image thermometry: the method and implementation. Exp Fluids 1:77–86

Ferraudi GJ (1988) Elements of inorganic photochemistry. Wiley, New York

Gendrich CP, Koochesfahani MM, Nocera DG (1997) Molecular tagging velocimetry and other novel application of a new phosphorescent supramolecule. Exp Fluids 23:361–372

Gendrich CP, Koochesfahani MM (1996) A spatial correlation technique for estimating velocity fields using molecular tagging velocimetry (MTV). Exp Fluids 22:67–77

Hartmann WK, Gray MHB, Ponce A, Nocera DG (1996) Substrate induced phosphorescence from cyclodextrin lumophore host-guest complexes. Inorg Chim Acta 243:239

Hu H, Koochesfahani MM (2003) A novel technique for quantitative temperature mapping in liquid by measuring the lifetime of laser induced phosphorescence. J Visualization 6(2):143–153

Kim HJ, Khim KD (2001) Application of a two-color laser induced fluorescence (LIF) technique for temperature mapping. In: 2001 ASME International Mechanical Engineering Congress and Exposition, November 11–16, 2001, New York

Koochesfahani MM, Cohn RK, Gendrich CP, Nocera DG (1996) Molecular tagging diagnostics for the study of kinematics and mixing in liquid phase flows. In: Proceedings of the Eighth International Symposium on Applications of Laser Techniques to Fluids Mechanics, July 8–11, 1996, Lisbon, vol. I, 1.2.1–1.2.12; Also in Developments in Laser Techniques and Fluid Mechanics, Chapter 2, section 1, p. 125, Eds. Adrian, Durao, Durst, Maeda, and Whitelaw; Springer, Berlin, Heidelberg, New york 1997

Lavieille P, Lemoine F, Lavergne G, Lebouche M (2001) Evaporating and combusting droplet temperature measurements using two-color laser-induced fluorescence. Exp Fluids 31(1):45–55

Mortellaro MA, Nocera DG (1996) A turn-on for optical sensing. Chem Technol 26:17–23

Ponce A, Wong PA, Way JJ, Nocera DG (1993) Intense phosphorescence trigged by alcohol upon formation of a cyclodextrin ternary complex. J Phys Chem 97:11137

Pringsheim P (1949) Fluorescence and phosphorescence. Interscience Publishers, INC. New York

Saeki S, Hart DP (2001) Investigation on YAG (532) laser dyes for oil film thickness and temperature measurement. In: Proceedings of the third pacific symposium of flow visualization and image processing (Paper index number F3096), March 18–21, 2001, Maui, Hawaii

Sakakibara J, Hishida K, Maeda M (1993) Measurements of thermally stratified pipe flow using image-processing techniques. Exp Fluids 16(2):82–96

Sakakibara J, Adrian RJ (1999) Whole-field measurement of temperature in water using two-color laser induced fluorescence. Exp Fluids 26(1):7–15

Sato K, Kasagi N, Suzuki, Y (1997) Combined velocity and scalar field measurement with the simultaneous use of PIV and scanning LIF. In: Proceedings of 10th international symposium on transport phenomena in thermal science and process engineering, Kyoto, Vol. 2:541–546

Thomson SL, Maynes D (2001) Spatially resolved temperature measurement in a liquid using laser induced phosphorescence. J Fluid Eng 123:293–302

Turro NJ (1978) Modern Molecular Photochemistry. Benjamin/Cummings, Menlo Park